Paradigm change in 3D inversion of airborne EM surveys: case study for oil sands exploration near Fort McMurray, Alberta

Michael S. Zhdanov,[1,2*] Leif Cox,[1] and Jonathan Rudd[3] demonstrate with a case study of oil sands exploration near Fort McMurray, Alberta how the 3D inversion of airborne electromagnetic survey data can be used to improve near-surface imaging, in their view a potential paradigm change particularly with regard to hydrocarbon exploration.

Over the last decade, airborne electromagnetic (AEM) systems have evolved on different platforms with different configurations of ever-increasing moments, and processing technologies have improved data quality significantly. In particular, helicopter time-domain electromagnetic (HTEM) systems such as AeroTEM, HELITEM, SkyTEM, and VTEM have dominated the AEM industry for mineral exploration and environmental studies. Yet AEM methods have generally had very limited use in hydrocarbon exploration. Recent interest in AEM has been driven by the requirement for a cost-effective method for the characterization and environmental due diligence of surface-mineable oil sands and shallow, steam-assisted gravity drainage (SAGD) prospects near Fort McMurray, Alberta, Canada. The primary advantage of AEM is that hundreds to thousands of line kilometres of high resolution, multichannel EM data can be rapidly and safely acquired over large areas with zero surface disturbances and at a fraction of the cost of seismic reflection.

To date, various AEM data acquired for oil sands exploration have been interpreted using conductivity depth images or layered-earth models for each transmitter-receiver pair (e.g., Kellett and Maris, 2002; Cristall et al., 2004; Huang and Rudd, 2008; McConnell and Glenn, 2008; Smith et al., 2008; Walker and Rudd, 2008). These 1D resistivity models are often stitched or interpolated in order to produce a pseudo-3D model over the survey area. However, the geological structures of particular interest to oil sands exploration, such as faults, paleochannels, and variable oil sand and groundwater distributions, are poorly resolved with these various 1D methods, and the geological structures often manifest themselves ambiguously within artifacts or distortions in the 1D-derived pseudo-3D models. Moreover, for coincident loop HTEM systems (e.g., AeroTEM, SkyTEM, VTEM), only the vertical component can be processed with all of the various 1D methods, as the predicted in-line component is identically zero above a layered-earth model. Yet, the measured in-line component contains important information about 3D resistivity variations that is not contained in the vertical component.

The primary problem with 3D AEM forward modeling is the necessity to solve as many linear systems of equations as there are transmitter positions in the survey. In the case of 3D AEM inversion, this problem is exacerbated by the need to compute Fréchet derivatives and repeating the whole process for multiple iterations. Cox and Zhdanov (2007) and Cox et al. (2010) introduced the concept of 3D AEM inversion with a moving sensitivity domain. According to this concept, one needs only to calculate the AEM responses and sensitivities for that part of the 3D earth model that is within the AEM system's sensitivity domain for a particular transmitter-receiver pair. These sensitivities are then superimposed for all transmitter-receiver pairs into a single, sparse sensitivity matrix for the entire 3D earth model. This approach has resulted in a paradigm change for AEM data interpretation. It makes it possible within a day, on high-end workstations, to invert entire AEM surveys with no approximations into high resolution 3D earth geoelectrical models. We demonstrate this with a case study of the 3D inversion of AeroTEM IV data for oil sands exploration near Fort McMurray. Our 3D inversion results show AEM's ability to map geological hazards such as paleochannels, as well as oil sands.

3D AEM inversion

The concept of a moving sensitivity domain for computing both AEM responses and sensitivities was introduced by Cox and Zhdanov (2007). By doing so, the authors were able to increase the AEM problem size by nearly five orders of magnitude (Wilson et al., 2012). Using a similar moving sensitivity domain methodology, Cox et al. (2010) applied the full IE

[1] *Technoimaging, 4001 South, 700 East, Suite 500, Salt Lake City, UT 84107, USA*
[2] *University of Utah, 1450 East, 100 South Salt Lake City, UT 84102, USA.*
[3] *Quantec Geoscience, 146 Sparks Ave, Toronto, Ontario M2H 2S4, Canada.*
[*] *Corresponding author, E-mail: mzhdanov@technoimaging.com*

method for both modelling and calculating the sensitivities of the frequency-domain AEM data. As a result, the Fréchet matrix is constructed as a sparse matrix with memory and computational requirements reduced by several orders of magnitude. The number of non-zero elements in each row of the sensitivity matrix is just the number of elements within each sensitivity domain (in an order of thousands) rather than the total number of elements in the domain (in the order of hundreds of thousands or millions).

Our frequency-domain modelling is based on the 3D contraction integral equation method and the generalized minimal residual algorithm of matrix inversion, which ensures rapid and robust computer simulation of the AEM data (Hursán and Zhdanov, 2002). For time-domain AEM, system responses and sensitivities are obtained by Fourier transforms of the frequency-domain responses and sensitivities, and are convolved with the transmitter waveform and integrated over the receiver windows (Raiche, 1998; Cox et al., 2012). We use a regularized conjugate gradient method for minimizing the Tikhonov parametric functional with either smooth or focusing stabilizers (Zhdanov, 2002) to produce the inverse images with relatively sharp boundaries between different geological formations. We refer interested readers to Zhdanov (2002, 2009) for further details.

Case study: Fort McMurray, Alberta, Canada

A typical geological section of the Fort McMurray area in Alberta, Canada, with the associated resistivity, is presented in Figure 1. The more resistive McMurray Formation sandstones tend to correlate with richer oil sands. However, the McMurray Formation can vary in both thickness and oil in place, and can contain conductive mudstone horizons. Locally, the overburden and/or Clearwater Formation shale units may or may not be present. If they are present, they may not be continuous. The Devonian limestone basement is generally resistive, but local increases in conductivity with depth can be attributed to the presence of saline groundwater and/or clays at the contact between the McMurray Formation and the basement. As employed in an inductive electromagnetic method, AEM data are more sensitive to conductive formations and fluids than resistive ones. Unlike other AEM applications, this implies that subtle trends in the data need to be discerned for recovering 3D resistivity variations in the McMurray Formation. Furthermore, this underscores the importance of understanding the actual AEM system parameters required for quantitative interpretation.

AeroTEM system description

AeroQuest optimized its AeroTEM system (now AeroTEM IV) to provide the maximum amount of information on the subsurface resistivity, and detail its system parameters for subsequent quantitative interpretation. The transmitter consists of a large loop towed by a helicopter with in-line and vertical receivers located at the centre of the transmitter loop. The diameter of the transmitter loop can be 5 m, 9 m, or 12 m. The transmitter waveform is a bipolar, symmetric triangular pulse which can be operated at 30 Hz, 90 Hz, or 150 Hz base frequencies with a 30% to 50% duty cycle. The transmitter moment is 4 x 10^4 Am^2 for the 5 m AeroTEM system, and 2.3 x 10^5 Am^2 for the 12 m AeroTEM system. The in-line and vertical components of the induced voltage of the secondary magnetic fields are measured during both the transmitter on- and off-times. There are 16 on-time channels and 17 off-time channels for both components. Finite transmitter turn-off time may affect TEM data at early times shortly after transmitter turn-off when the transmitter turn-off time is large. The AeroTEM system allows sufficient time between the transmitter turn-off and the first time-off data sampling to avoid the effects of transmitter turn-off.

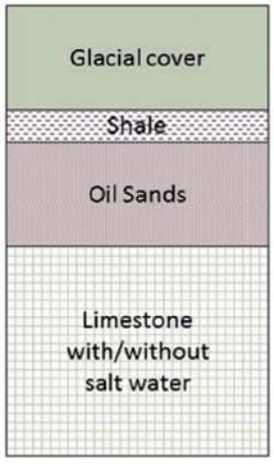

Geologic Unit	Resistivity (Ωm)	Thickness (m)
Overburden	100's	0 – 200
Clearwater Formation	2-10	0 – 30
McMurray Formation	100 – 1000	50 – 100
Devonian Basement	1 – 1000	N/A

Figure 1 *Typical geological section and related resistivity properties for the Fort McMurray area, Alberta.*

3D AeroTEM inversion

We consider a 175 line km survey of AeroTEM IV data acquired over an oil sands prospect near Fort McMurray that was conducted as a demonstration survey for Husky Oil. Paleochannels are clearly obvious in the data (e.g., Figure 2). For quantitative interpretation, the data were inverted for a 3D resistivity model using the moving sensitivity domain method described by Cox et al. (2012). As can be seen in Figure 2, the predicted data have been able to capture the subtle trends of the observed data. Figure 3 shows the resulting 3D resistivity model. Note that, the inversion was able to recover the resistive (i.e., probably freshwater filled) paleochannel in glacial till, and the conductive Clearwater shale layer. The top of the McMurray formation can be recovered in parts of the survey area as well.

Figure 4 presents a comparison between a geological map and resistivity depth section at 10 m, obtained by 3D inversion of the AeroTEM IV data over the Fort McMurray area. The red line superimposed on the resistivity depth section shows the contour of the paleochannel in glacial till, mapped by geological data. One can see that this paleochannel is manifested by high resistivity in the horizontal section of the 3D inverse geoelectrical model.

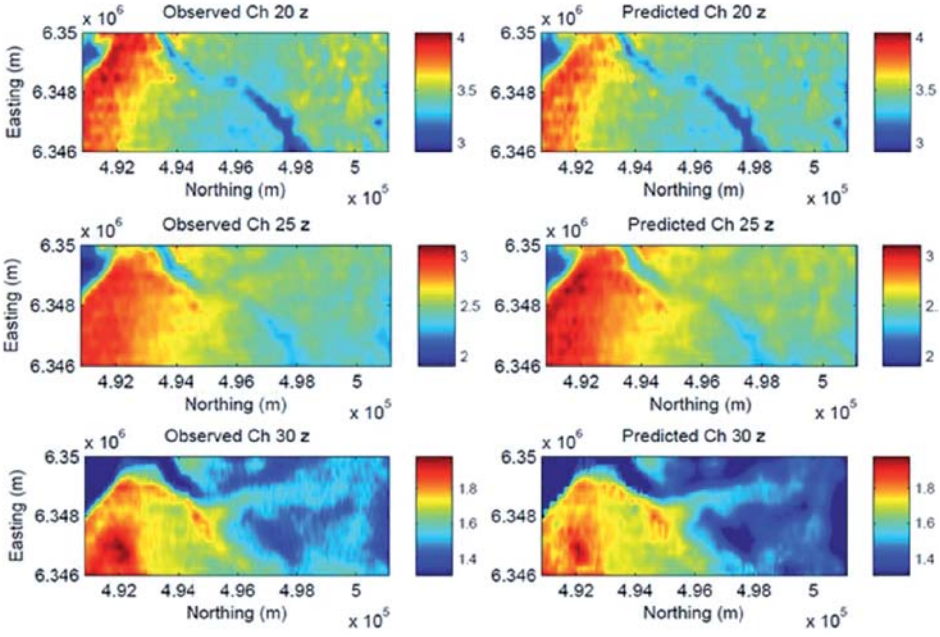

Figure 2 *Examples of the observed (left) and predicted (right) data for different channels of the vertical component from the AeroTEM IV survey over the Fort McMurray area.*

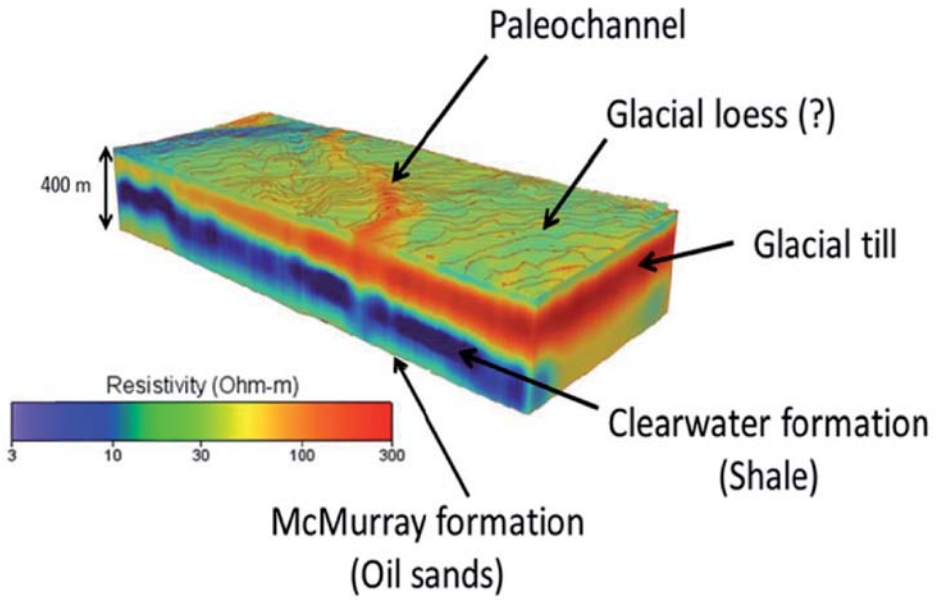

Figure 3 *3D resistivity model obtained from 3D inversion of the 175 line km of AeroTEM IV data. Note that the inversion was able to recover the paleochannel in glacial till, the Clearwater formation, and the top of the McMurray formation.*

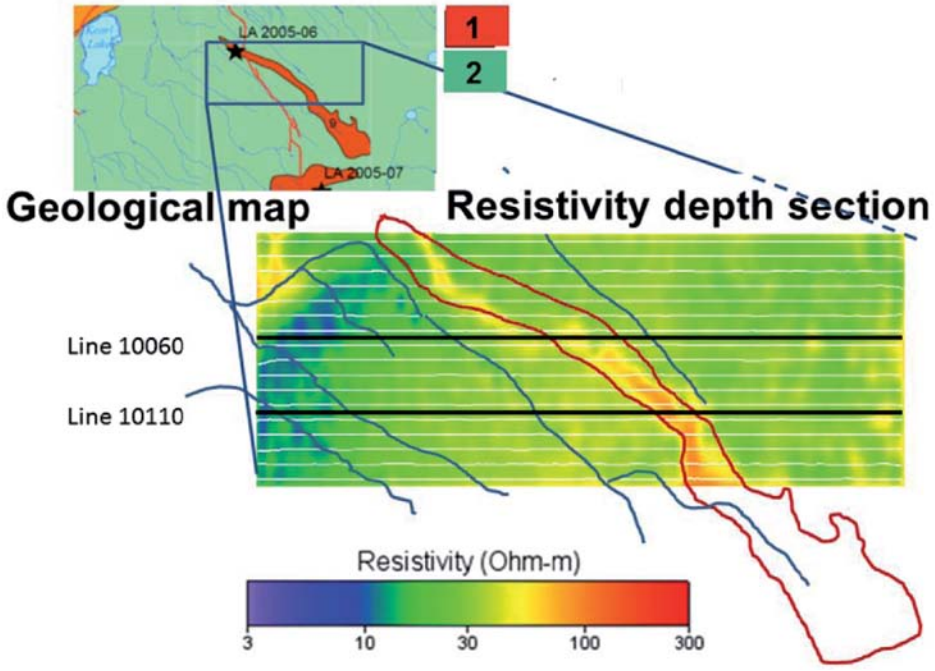

Figure 4 *Comparison of geological map and resistivity depth section at 10 m, obtained by 3D inversion of the AeroTEM IV data over the Fort McMurray area: 1) Meltwater-channel sediments; 2) Hummocky moraine. The red line superimposed on the resistivity depth section shows the contour of the paleochannel in glacial till from geological data. The solid black lines show the location of the survey lines 10060 and 10110 superimposed on the resistivity depth section. Vertical resistivity cross sections for these lines are shown in Figure 5.*

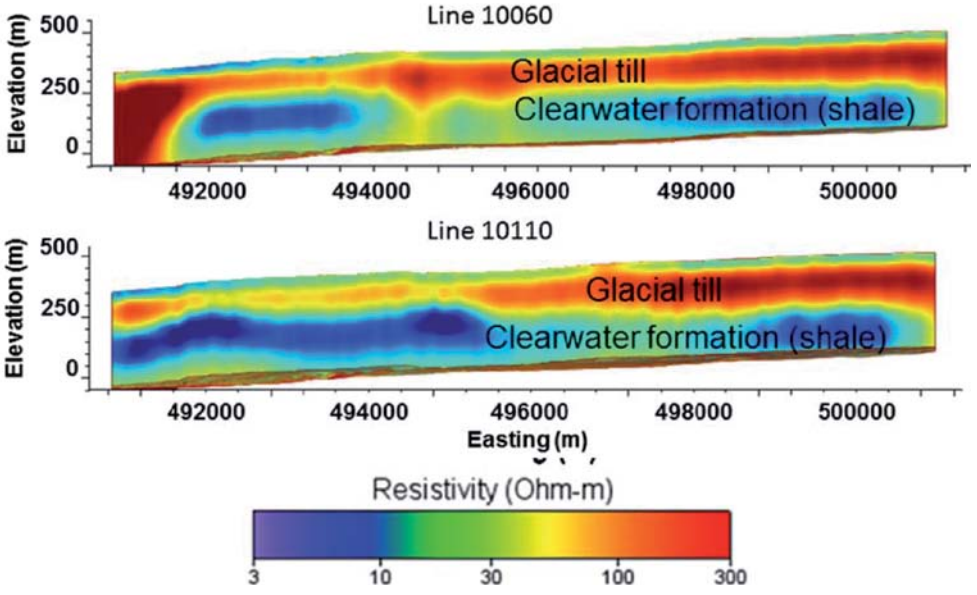

Figure 5 *Vertical resistivity cross sections of the 3D resistivity model obtained from 3D inversion of AeroTEM IV data for lines 10060 and 10110 shown in Figure 4. One can clearly see the resistive glacial till layer at the top, the conductive Clearwater formation (shale) in the middle, and the resistive McMurray formation (oil sands) at the bottom of the resistivity sections, respectively.*

Figure 5 presents vertical resistivity cross sections of the inverse model for the survey lines 10060 and 10110 shown in Figure 4. We can clearly see the resistive glacial till layer at the top, the conductive Clearwater formation (shale) in the middle, and the resistive McMurray formation (oil sands) at the bottom of the resistivity sections, respectively.

Conclusions

We demonstrate in this paper that the development of the concept of moving sensitivity domain has resulted in a paradigm change in 3D inversion of AEM data. This opens a possibility for application of the AEM data to the solution of challenging problems of subsurface imaging typical for HC exploration. We have presented the results from the 3D inversion of 175 line km of AeroTEM IV data from an oil sands prospect near Fort McMurray, Alberta. The model produced from our full 3D inversion has been able to image the near-surface paleochannel with better resolution than various 1D methods. We note that the accurate imaging of such structures is critical for geological hazard identification and mine planning. The 3D inversion has also been able to image the near-surface glacial loess, glacial till, and the Clearwater and McMurray forma-

tions. Further analysis and integration of the 3D inversion results with other geological information is ongoing.

Acknowledgements

The authors acknowledge TechnoImaging and AeroQuest for support of this research and permission to publish. Zhdanov also acknowledges support of the University of Utah's Consortium for Electromagnetic Modeling and Inversion (CEMI).

References

Cox, L. H. and Zhdanov, M. S. [2007] Large-scale 3D inversion of HEM data using a moving footprint. *77th SEG Annual Meeting*, San Antonio, Texas.

Cox, L. H., Wilson, G. A. and Zhdanov M. S. [2010] 3D inversion of airborne electromagnetic data using a moving footprint. *Exploration Geophysics*, **41**, 250–259.

Cox, L.H., Wilson, G.A., and Zhdanov, M.S. [2012] 3D inversion of airborne electromagnetic data. *Geophysics*, **77** (4), WB59-WB69.

Cristall J., Farquharson, C. and Oldenburg, D. [2004] Airborne electromagnetic inversion applied to oil sands exploration. *CSEG National Convention*, Calgary.

Huang, H. and Rudd, J. [2008] Conductivity-depth imaging of helicopter-borne TEM data based on a pseudolayer half-space model. *Geophysics*, **73**, F115–F120.

Hursán, G. and Zhdanov, M. S. [2002] Contraction integral equation method in three-dimensional electromagnetic modeling. *Radio Science*, **37**, 1086.

Kellett, R. L. and Maris, V. [2002] Imaging electrically resistive oil sand channels in northeast Alberta, Canada. *16th IAGA Workshop on Electromagnetic Induction in the Earth*, Santa Fe, New Mexico.

McConnell, D. and Glenn, T. [2008] Athabasca oil sands exploration and development investigation using the helicopter-borne transient electromagnetic technique. *CSPG–CSEG–CWLS Convention*, Calgary.

Raiche, A. [1998] Modelling the time-domain response of AEM systems. *Exploration Geophysics*, **29**, 103–106.

Smith, R., McConnell, D. and Rowe, J. [2008] The application of airborne electromagnetics to hydrocarbon exploration. *First Break*, **26** (11), 65–70.

Walker, S. and Rudd, J. [2008] Airborne resistivity mapping with helicopter TEM: An oil sands case study. *5th International Conference on Airborne Electromagnetics*, Haikko Manor, Finland.

Wilson, G.A., Cox, L.H., Cuma, M. and Zhdanov, M.S. [2012] Inverting airborne geophysical data for mega-cell and giga-cell 3D Earth models. *The Leading Edge*, **31** (3), 316–321.

Zhdanov, M.S. [2002] *Geophysical inverse theory and regularization problems*. Elsevier, Amsterdam.

Zhdanov, M.S. [2009] *Geophysical electromagnetic theory and methods*. Elsevier, Amsterdam.